QUANTUM SUPERPOSITIONS AND DECOHERENCE: HOW TO DETECT INTERFERENCE OF MACROSCOPICALLY DISTINCT OPTICAL STATES

F. T. ARECCHI

Department of Physics, University of Florence, Florence, Italy; and National Institute of Applied Optics (INOA), Florence, Italy

A. MONTINA

Department of Physics, University of Florence, Florence, Italy

CONTENTS

I. Quantum Superposition and Decoherence
II. Optical Implementation of Mesoscopic Quantum Interference
III. "Which Path" Experiment with a Large Photon Number
Acknowledgment
References

I. QUANTUM SUPERPOSITION AND DECOHERENCE

There is a basic difference between the predictions of quantum theory for quantum systems that are closed (isolated) and open (interacting with their environments.) In the case of a closed system, the Schrödinger equation and the superposition principle apply literally. In contrast, the superposition principle is not valid for open quantum systems. Here the relevant physics is quite different, as has been shown by many examples in the context of condensed matter physics,

Dynamical Systems and Irreversibility: A Special Volume of Advances in Chemical Physics, Volume 122, Edited by Ioannis Antoniou. Series Editors I. Prigogine and Stuart A. Rice.
ISBN 0-471-22291-7.

quantum chemistry, and so on. The evolution of open quantum systems has to be described in a way violating the assumption that each state in the Hilbert space of a closed system is equally significant. Decoherence is a negative selection process that dynamically eliminates nonclassic states.

The distinguishing feature of classic systems, the essence of "classic reality," is the persistence of their properties—the ability of systems to exist in predictably evolving states, to follow a trajectory which may be chaotic, but is deterministic. This suggests the relative stability—or, more generally, predictability—of the evolution of quantum states as a criterion that decides whether they will be repeatedly encountered by an observer and can be used as ingredients of a "classic reality." The characteristic feature of the decoherence process is that a generic initial state will be dramatically altered on a characteristic decoherence time scale: Only certain stable states will be left on the scene.

Quantum measurement is a classic example of a situation in which a coupling of a macroscopic quantum apparatus A and a microscopic measured system S forces the composite system into a correlated, but usually exceedingly unstable, state. In a notation where $|A_0\rangle$ is the initial state of the apparatus and $|\psi\rangle$ the initial state of the system, the evolution establishing an A–S correlation is described by

$$|\psi\rangle|A_0\rangle = \sum_k \alpha_k|\sigma_k\rangle|A_0\rangle \rightarrow \sum_k \alpha_k|\sigma_k\rangle|A_k\rangle = |\Phi\rangle \tag{1}$$

An example is the Stern–Gerlach apparatus. There the states $|\sigma_k\rangle$ describe orientations of the spin, and the states $|A_k\rangle$ are the spatial wavefunctions centered on the trajectories corresponding to different eigenstates of the spin. When the separation of the beams is large, the overlap between them tends to zero ($\langle A_k|A'_k\rangle \sim \delta_{kk'}$). This is a precondition for a good measurement. Moreover, when the apparatus is not consulted, A–S correlations would lead to a mixed density matrix for the system S:

$$\rho_s = \sum_k |\alpha_k|^2|\sigma_k\rangle\langle\sigma_k| = Tr|\Phi\rangle\langle\Phi| \tag{2}$$

However, this premeasurement quantum correlation does not provide a sufficient foundation to build a correspondence between the quantum formalism and the familiar classic reality. It only allows for Einstein–Podolsky–Rosen quantum correlations between A and S, which imply the entanglement of an arbitrary state—including nonlocal, nonclassic superpositions of the localized status of the apparatus (observer)—with the corresponding relative state of the other system. This is a prescription for a Schrödinger cat, not a resolution of the

measurement problem. What is needed, therefore, is an effective superselection rule that "outlaws" superpositions of these preferred "pointer states." This rule cannot be absolute: There must be a time scale sufficiently short, or an interaction strong enough, to render it invalid, because otherwise measurements could not be performed at all. Superselection should become more effective when the size of the system increases. It should apply, in general, to all objects and allow us to reduce elements of our familiar reality—including the spatial localization of macroscopic system—from Hamiltonians.

Environment-induced decoherence has been proposed to fit these requirements [1]. The transition from a pure state $|\Phi\rangle\langle\Phi|$ to the effectively mixed ρ_{AS} can be accomplished by coupling the apparatus A to the environment ϵ. The requirement to get rid of unwanted, excessive, EPR-like correlations (1) is equivalent to the demand that the correlations between the pointer states of the apparatus and the measured system ought to be preserved in spite of an incessant measurement-like interaction between the apparatus pointer and the environment. In simple models of the apparatus, this can be assured by postulating the existence of a pointer observable with eigenstates (or, more precisely, eigenspaces) that remain unperturbed during the evolution of the open system. This "nondemolition" requirement will be exactly satisfied when the pointer observable O commutes with the total Hamiltonian generating the evolution of the system:

$$[(H + H_{\text{int}}), O] = 0 \tag{3}$$

For an idealized quantum apparatus, this condition can be assumed to be satisfied and—provided that the apparatus is in one of the eigenstates of O—leads to an uneventful evolution:

$$|A_k\rangle|\epsilon_0\rangle \rightarrow |A_k\rangle|\epsilon_k(t)\rangle \tag{4}$$

However, when the initial state is a superposition corresponding to different eigenstates of O, the environment will evolve into an $|A_k\rangle$-dependent state:

$$\left(\sum_k \alpha_k|A_k\rangle\right)|\epsilon_0\rangle \rightarrow \sum_k \alpha_k|A_k\rangle|\epsilon_k(t)\rangle \tag{5}$$

The decay of the interference terms is inevitable. The environment causes decoherence only when the apparatus is forced into a superposition of states, which are distinguished by their effect on the environment. The resulting continuous destruction of the interference between the eigenstates of O leads to an effective environment-induced superselection. Only states which are stable in spite of decoherence can exist long enough to be accessed by an observer so that they can count as elements of our familiar, reliably existing reality.

Effective reduction of the state vector follows immediately. When the environment becomes correlated with the apparatus,

$$|\Phi\rangle|\epsilon_0\rangle \rightarrow \sum_k \alpha_k |A_k\rangle|\sigma_k\rangle|\epsilon_k(t)\rangle = |\Psi\rangle \tag{6}$$

but the apparatus is not consulted (so that it must be traced out), we have

$$\rho_{AS} = \mathrm{Tr}|\Psi\rangle\langle\Psi| = \sum_k |\alpha_k|^2 |A_k\rangle\langle A_k| \, |\sigma_k\rangle\langle\sigma_k| \tag{7}$$

Only correlations between the pointer states and the corresponding relative states of the system retain their predictive validity. This form of ρ_{AS} follows, provided that the environment becomes correlated with the set of states $\{|A_k\rangle\}$ (it could be any other set) and that it has acted as a good measuring apparatus, so that $\langle\epsilon_k(t)|\epsilon_{k'}(t)\rangle = \delta_{kk'}$ (the states of the environment and the different outcomes are orthogonal).

Let us consider a system S ruled by a Hamiltonian H_0 and coupled to the environment through the term

$$H' = \nu x E \tag{8}$$

where ν is the coupling strength, x is a coordinate of the system, and E is an environment operator. As we trace the overall density operator over an ensemble of environments with temperature T, the system's density matrix in the coordinate representation, $\rho(x, x')$, evolves according to the following master equation [2]:

$$\frac{d\rho}{dt} = \frac{1}{i\hbar}[H_0, \rho] - \gamma(x - x')(\partial_x - \partial_{x'})\rho - \eta\frac{kT}{\hbar^2}(x - x')^2\rho \tag{9}$$

where $\eta := \nu^2/2$, and $\gamma := \eta/2m$ is the drift coefficient that rules the evolution of the first moments. "Negative selection" consists of the rapid decay of the off-diagonal elements of $\rho(x, x')$. Indeed, for $\hbar \rightarrow 0$, the last term on the right-hand side of (9) prevails, providing the solution

$$\rho(x, x', t) = \rho(x, x', 0)\exp\left(-\eta\frac{kT}{\hbar^2}(x - x')^2\right) \tag{10}$$

With $\Delta x = x - x'$, we see that an initial offset $\rho(x, x', 0)$ decays after a decoherence time

$$\tau_D = \frac{1}{\gamma}\left(\frac{\lambda_{DB}}{\Delta x}\right)^2 \tag{11}$$

where

$$\lambda_{DB} = \frac{\hbar}{p} = \frac{\hbar}{\sqrt{2mkT}} \tag{12}$$

is the thermal de Broglie length. At length scales $\Delta x \gg \lambda_{DB}$, we have $\tau_D \ll 1/\tau$, such that the system decoheres rapidly and then continues with the standard Brownian decay on the time scale $1/\gamma$.

II. OPTICAL IMPLEMENTATION OF MESOSCOPIC QUANTUM INTERFERENCE

The possibility of interference between macroscopically distinct states (the so-called Schrödinger cats [3]) has been suggested by Leggett [4–6] for the case of two opposite magnetic flux states associated with a SQUID.

Recently, two experiments on Schrödinger cats have been demonstrated. In the first one [7] the two different states $|\pm\alpha\rangle$ are coherent states of the vibrational motion of a $^9Be^+$ion within a one-dimensional ion trap. The maximum separation reported between the two states corresponds to about $2|\alpha| = 6$. In the second one [8] the two different states are coherent states of a microwave field, with a maximum separation up to about 3.3.

An optical experiment would consist of generating the superposition of two coherent states of an optical field and detecting their interference. Generating a superposition of coherent states requires some nonlinear optical operations, and different proposals have been formulated, based respectively on $\chi^{(3)}$ and $\chi^{(2)}$ nonlinearities. In the first one [9] a coherent state, injected onto a $\chi^{(3)}$ medium, evolves toward the superposition of two coherent states 180° out of phase with each other. However, for all practically available $\chi^{(3)}$ values, the time necessary to generate the superposition state, which scales as $1/\chi^{(3)}$, is always much longer than the decoherence time. We recall that for a superposition $(|\alpha\rangle + |-\alpha\rangle)/\sqrt{2}$ of two coherent states, the decoherence time is given by the damping time of the field, divided by the square distance $(4|\alpha|^2)$ [9].

The second proposal, by Song, Caves, and Yurke (SCY) [10], consists of an optical parametric amplifier (OPA) pumped by a coherent field, generating an entangled state of signal (S) and readout (R) modes. Passing the S mode through a further OPA, and measuring its output field conditioned upon the photon number on the R mode, should yield interference fringes, associated with the coherent superposition of two separate states. However, the fringe visibility is extremely sensitive to the R detector efficiency, and as a result the SCY interference has not been observed so far.

We have recently introduced a modified version of SCY, whereby fringes can still be observed at the efficiencies of currently available detectors [11]. The

price to be paid is a very low count rate, which is, however, compensated for by the use of a high-frequency pulsed laser source. Our setup is shown in Fig. 1.

Choosing the back-evasion condition of Ref. 12 it can be shown that the state of the two field modes at the output of the first OPA apparatus is

$$|\psi\rangle = e^{-iT\hat{X}_S\hat{Y}_R}|0,0\rangle \tag{13}$$

where $T = 2\sinh(r)$, r being proportional to the product of the pump laser amplitude and the nonlinear susceptibility $\chi^{(2)}$ of the parametric amplifier [13], and $\hat{X}_S = (\hat{a}_S + \hat{a}_S^+)/\sqrt{2}, \hat{Y}_R = (\hat{a}_R - \hat{a}_R^+)/(i\sqrt{2})$.

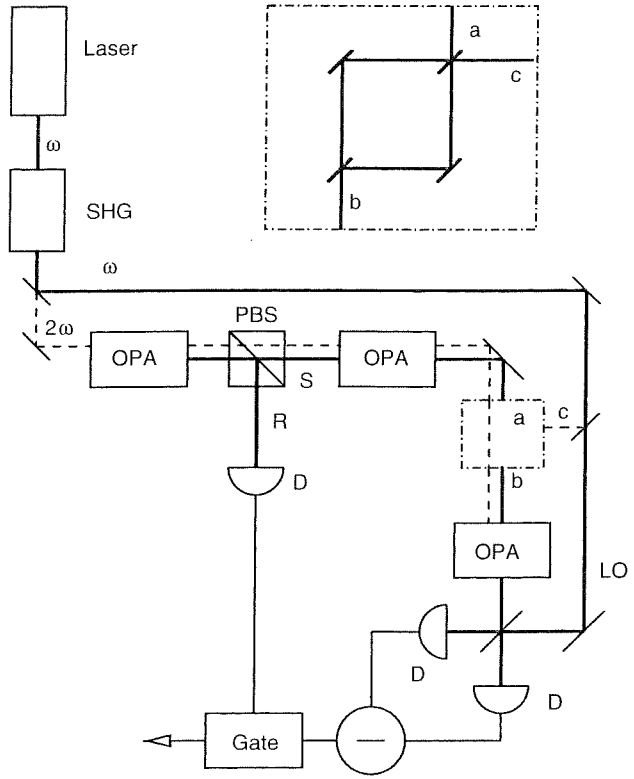

Figure 1. Layout of the proposed experiment: SHG, second harmonic generation; OPA, optical parametric amplifiers (including polarization rotators); PBS, polarizing beam splitter; R, readout channel; S, signal channel; D, detectors; LO, local oscillator for homodyne. The homodyne detection is performed via a balanced scheme. The dashed–dotted box on the S channel (magnified in the inset) denotes the optional insertion of a Mach–Zehnder interferometer with two inputs, a and c, and one output, b. Branch c include a phase adjustment in order to build the superposition state given by Eq. (25). When no interferometer is inserted, a coincides with b.

In the representation of the eigenstates $|x_S, y_R\rangle$ of $\hat{X}_S$ e $\hat{Y}_R$, $|\psi\rangle$ is written as

$$\psi(x_S, y_R) = \langle x_S, y_R|\psi\rangle = e^{-iTx_S y_R}\psi_o(x_S, y_R) \tag{14}$$

where $\psi_o(x_S, y_R)$ is the wavefunction of the vacuum state.

By a photodetection measurement on mode R, we obtain the (not normalized) state ψ_n^S of mode S conditioned upon the photon number n on R, that is,

$$\psi_n^S(x_S) = \int_{-\infty}^{\infty} dy_R \psi(x_S, y_R)\psi_n^*(y_R) \tag{15}$$

where n is the photon number detected on R and $\psi_n(y_R)$ is the number state $|n\rangle$ in the y_R representation of the R mode.

The integral

$$P(n) = \int_{-\infty}^{\infty} |\psi_n^S(x)|^2\, dx \tag{16}$$

gives the probability that n photons are in mode R.

The probability distribution of x_s, conditioned on the photon number in mode R, is [13]

$$P(x_S|n) = \frac{|\psi_n^S(x_S)|^2}{P(n)} = \frac{(2n)!!(1+T^2/2)^{(2n+1)/2}}{\pi^{1/2}n!(2n-1)!!} x_S^{2n} e^{-(1+T^2/2)x_S^2} \tag{17}$$

Both the dependence of $P(n)$ upon n [Eq. (16)] and the dependence of $P(x|n)$ upon x [Eq. (17)] for n between 0 and 10 have been visualized in Figs. 1 and 2 of Ref. 11.

For $n > 0$ the conditional probability (17) is approximated by the sum of two Gaussians whose distance increases with n. The width of each of the two peaks is smaller than that corresponding to a coherent state. SCY suggested to increase the peak separation by passing the S signal through a degenerate OPA, described by the evolution operator

$$U_1(r_1) = e^{-r_1(\hat{a}_S\hat{a}_S - \hat{a}_S^+\hat{a}_S^+)} \tag{18}$$

The output of this second OPA consists of the superposition of two near-coherent states.

When measuring the quadrature Y_S at the output of the second OPA for a fixed photon number n detected on the R channel, interference fringes should appear as a result of the superposition.

The probability distributions $P(y_S|n)$ of Y_S for n that goes from 0 to 10 and for $T = 3$ are reported in Fig. 5 of Ref. 11. Of course, if we sum up several of them with their weights $P(n)$, the interference fringes cancel out. From this fact, it is easily understood how critical the quantum efficiency of the R photodetector is.

Let us suppose that the R photodetector has an efficiency $\eta_R < 1$. For the time being, we refer to a single photomultiplier detector. Selecting the laser wavelength, the quantum efficiency of the photocatode can be $\eta_R = 0.05$. If n photons impinge on it, the probability of detecting m photons is given by the binomial distribution

$$P(m|n) = \binom{n}{m} \eta_R^m (1 - \eta_R)^{n-m} \tag{19}$$

Thus, the probability of y_S conditioned by the detection of m photons on R is given by

$$\begin{aligned} P_\eta(y_S|m) &= \sum_{n \geq m} P(y_S|n) P(n|m) \\ &= \sum_{n \geq m} \frac{P(y_S|n) P(m|n) P(n)}{N(m)} \end{aligned} \tag{20}$$

where $P(n)$ is given by Eq. (16) and the normalization factor in the denominator is $N(m) = \sum_n P(m|n)P(n)$.

The P_η are reported in Fig. 2, using the parameters chosen in [13] ($T = 3$), for some values of the efficiency and for m that goes from 1 to 5. With $\eta_R = 0.7$ the fringes practically disappear, and therefore no superposition is observed.

The last term of Eq. (20), based on Bayes theorem, says that in order to get the distribution of y_S, conditioned by the detection of m photons, we must consider all distributions $P(y_S|n)$ for $n \geq m$, each one weighted by the probability $P(n|m)$ of n photons when m of them have been counted. With the parameters considered in Ref. 13, $P(n|4)$ has the behavior reported in Fig. 3a (we have set $m = 4$). The uncertainty on n implies a reduction of the fringe visibility on y_S.

We aim at reducing the width of the distribution $P(n|m)$, based on the available efficiency of commercial detectors. The only parameter that we can change is the gain T of the first OPA. Reducing the value of gain T, the distribution $P(n)$ decays faster for increasing n. In Fig. 3b we have reported

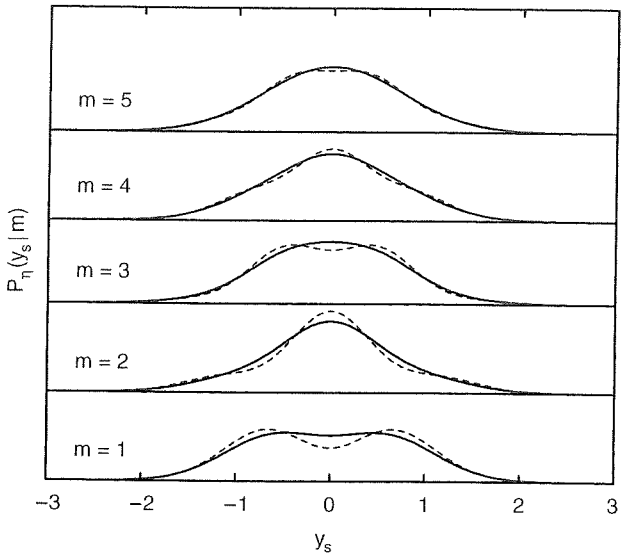

Figure 2. Probability distribution $P_\eta(y_S|m)$ of y_S for $T = 3$ and different efficiencies of the readout detector: $\eta_R = 0.7$ (dashed line), $\eta_R = 0.5$ (solid line).

$P(n|4)$ for $\eta_R = 0.3$ and for $T = 2,\ 1$, and 0.4. In this last case we note a sharp reduction of the probability for $n > m$; therefore if the detector counts m, there is a very small probability of having $n > m$ photons.

To confirm such a guess, we report in Fig. 4 the distributions $P_\eta(y_S|m)$ for some values of T and for $\eta_R = 0.3$.

The very remarkable fact is that for $T = 0.4$, the fringe visibility is not practically affected by lowering the quantum efficiency. An alternative detection scheme replaces the single photomultiplier with an array of single-photon detectors [14,15]. In such a case the binomial distribution (8) no longer holds, and one should instead recur to Eq. (11) of Ref. 12. This change does not affect the fringe visibility.

Lowering T has no practical influence on the separation of the two near-coherent states at the exit of the second OPA for the same photon number m in mode R.

However, there is a price to pay, indeed: A small T lowers the probability of photon detection on mode R. In Fig. 5 of Ref. 9 we have reported the distribution $N(m)$, for $\eta_R = 0.05$ and $T = 0.4$. $N(4)$ is less than 10^{-10}; thus even if we utilize a pulsed laser with frequency 80 MHz and select $m = 4$, we have less than one favorable event every 100 seconds.

Thus, we must compromise between the fringe visibility and the counting rate.

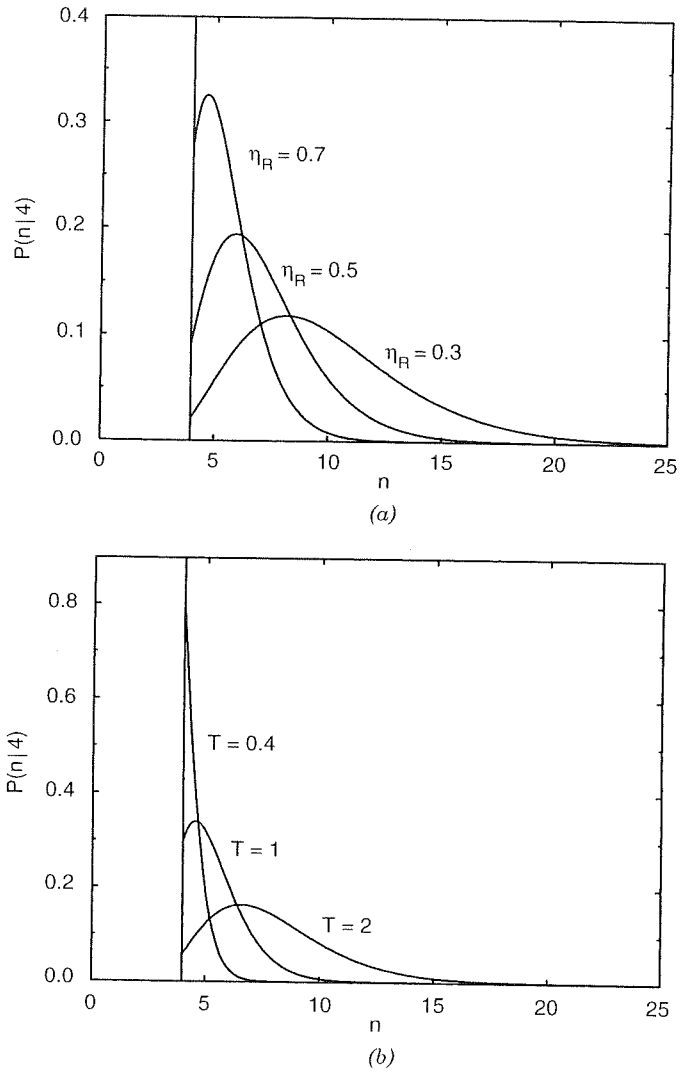

Figure 3. Conditional probability of an impinging photon number n when the detector registers $m = 4$ for (a) different efficiencies η_R at a fixed OPA gain $T = 3$ and (b) different gains T at a fixed efficiency $\eta_R = 0.3$.

A much higher counting rate is obtained by using an array of diodes following the proposal by Paul et al. [14,15]. For four photons, the count rate is now on the order of 10^{-6}, thus yielding 20–80 counts per second with a laser pulsed at an 80-MHz rate.

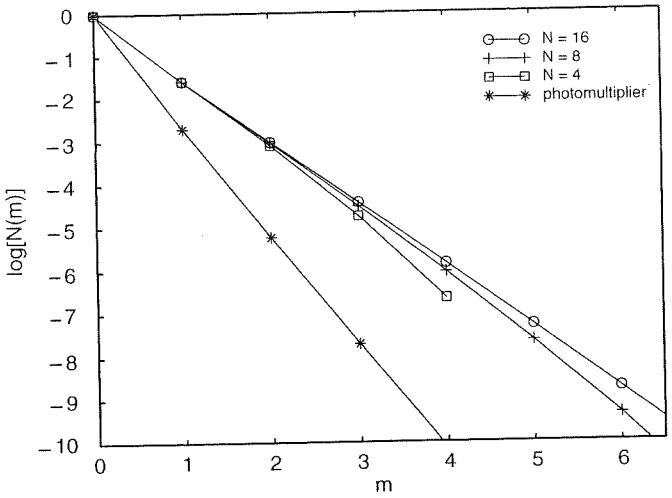

Figure 4. As Fig. 2 but with fixed $\eta_R = 0.3$, $T = 1$ (dashed line), and $T = 0.4$ (solid line).

The Y_S quadrature is measured via a homodyne detector. The mode S is superposed to a reference field at frequency ω, with appropriate phase, and we measure the intensity of the superposition.

The probability that the S detector counts N photons in the resulting field, if its efficiency is 1, is given by

$$P_o(N) = \left| \int_{-\infty}^{+\infty} \langle N|y_S\rangle \psi(y_S - A)\, dy_S \right|^2 \tag{21}$$

Accounting for the photodetector efficiency $\eta_S < 1$, the count probability becomes

$$P_o^{\eta}(M) = \sum_{N \geq M} P_o(N) P(M|N) \tag{22}$$

where

$$P(M|N) = \binom{N}{M} \eta_S^M (1 - \eta_S)^{N-M} \tag{23}$$

In Fig. 5a we report the distributions $P_o^{\eta}(M)$ for some values η_S of the homodyne detector efficiency in the case of a superposition of two coherent states of opposite phase with separation $2|\alpha| = 2\sqrt{5}$. For $\eta_S = 0.8$ the fringes are barely visible.

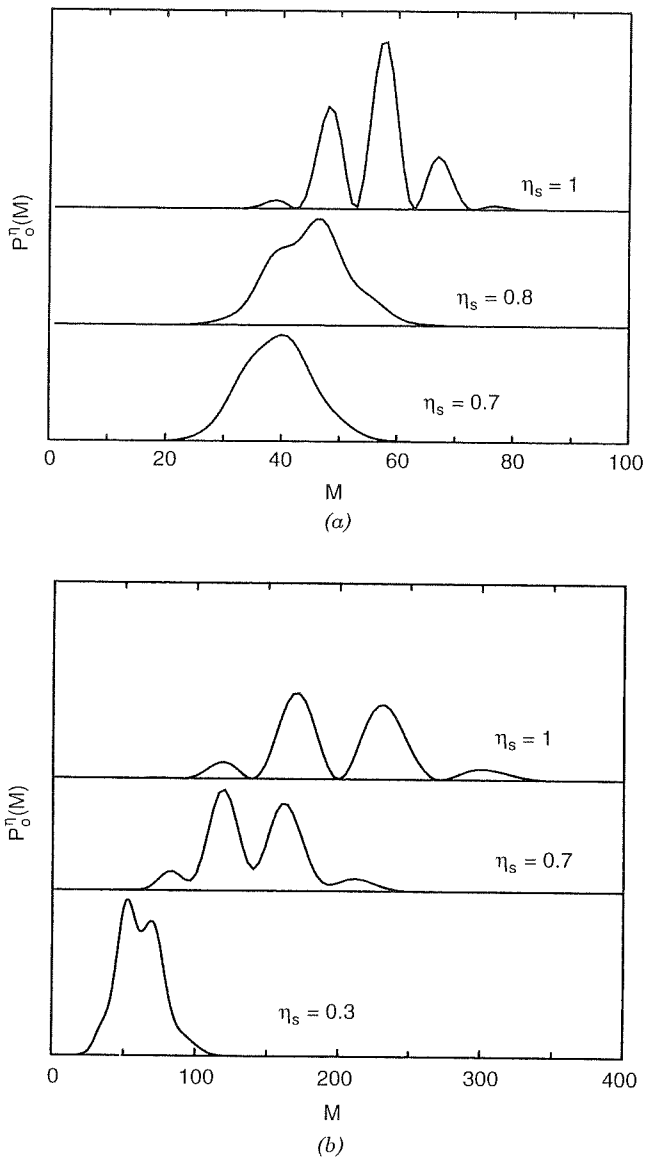

Figure 5. Photocount distribution after the homodyne detection for an input field of two coherent states $|\pm\alpha\rangle$ where $|\alpha|^2 = 5$ for different homodyne detector efficiencies η_S and with a pre-OPA set at different gains l: (a) $l = 1$ (no pre-OPA), (b) $l = 0.3$, (c) $l = 0.15$. The different horizontal scales correspond to different LO intensity for the three cases.

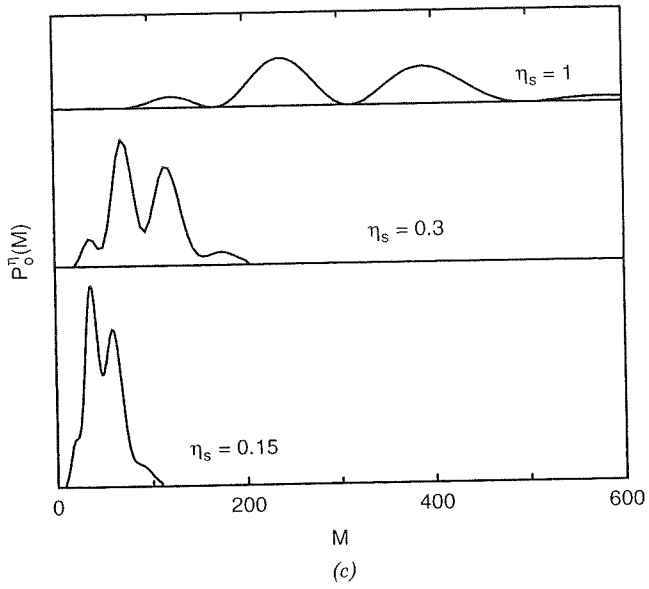

Figure 5. (*Continued*)

We expect that use of PIN diodes should provide a high detection efficiency [16]. However, we devise a way to improve the fringe visibility as if the efficiency were very close to unity.

$P(M|N)$ has the effect of rounding off the distribution $P_o(N)$. By spreading the distribution $P_o(N)$, it becomes less sensitive to this roundoff. This can be done by incorporating in the detection system a pre-OPA whose role consists in separating the fringes.

Indeed, the decoherence rate is proportional to the square root of the distance between the two states in the phase plane; thus an auxiliary OPA before the homodyne, with gain less than unity for the x_S quadrature, reduces the separation and therefore reduces the effect of the losses.

If $l(<1)$ is the shrinking factor for x_S in the auxiliary OPA, then the probability $P_o(N)$ of Eq. (21) changes to

$$P_o(N) = \left| \int_{-\infty}^{+\infty} \langle N|y_S\rangle \psi[l(y_S - A)]\, dy_S \right|^2 \tag{24}$$

The corresponding distributions $P_o^\eta(M)$ are reported for $l = 0.3$ and 0.15 in Figs. 5b and 5c, respectively, for the case $|\alpha|^2 = 5$. With $l = 0.3$ and $\eta_S = 0.7$ the fringes are well visible, confirming the validity of the proposed strategy.

Notice that Fig. 5 is evaluated for a photon number around 100, for sake of demonstration; in fact, the experiment is carried with a much higher LO intensity.

To summarize, the opposite roles of second and third OPA consist, respectively, of putting the two states of the superposition away and then reapproaching them. This means that a measurement done in the intermediate space region would resolve two widely separate states. The setup here proposed is an optical implementation of the ideal experiment suggested for the same purpose by Wigner in the case of two spin 1/2 particles, by use of two Stern–Gerlach apparatuses [17].

III. "WHICH PATH" EXPERIMENT WITH A LARGE PHOTON NUMBER

The availability of an intermediate spatial region suggests a way of transforming the phase-space separation of the two states of the superposition into a real space separation. Precisely, we might insert a Mach–Zehnder interferometer between second and third OPA. The two inputs of the first beam splitter are fed, respectively, by the superposition state $(|\alpha\rangle + |-\alpha\rangle)/\sqrt{2}$ and by a coherent state $|\gamma\rangle$ with $|\gamma| = |\alpha|$ and adjustable phase. By a suitable choice of this phase, the two separate arms A and B of the interferometer have a field given by the superposition

$$|\beta_1\rangle_A|0\rangle_B + |0\rangle_A|\beta_2\rangle_B \tag{25}$$

where $|\beta_1| = |\beta_2| = \sqrt{2}|\alpha|$.

Thus, a photodetection performed on the two arms of the interferometer would provide a photon number $2|\alpha|^2$ on one arm and 0 on the other or viceversa; however, if no measurement is performed within the interferometer, the homodyne system at the output will detect an interference between the two alternative paths. Adjusting the two interference arm lengths, we recover the input states at interferometer output. This final measurement is a "which path" experiment, upgraded to a packet of $2|\alpha|^2$ photons. So far this experiment had been performed with only one photon, whereas in our setup it is scaled to a large photon number.

The corresponding experiment is being carried at the National Institute of Applied Optics (INOA) in Florence, Italy.

A first run, with an Nd:YAG mode locked laser at $\lambda = 1.06\,\mu m$, was hampered by the low efficiency of available avalanche Si detectors at that wavelength. An improved version, using a Ti:Sa laser at $\lambda = 800\,nm$, provides a much better matching within the peak efficiency of the Si detectors. Preliminary reconstructions of the Wigner function of the superposition state have already tested the soundness of the proposed scheme.

Acknowledgment

This work was partly supported by INFM through the Advanced Research Project CAT.

References

1. Zurek, *Phys. Rev.* **D26**, 1862 (1982); *Phys. Today* **Oct.**, 36–44 (1991) and several comments regarding this article in *Phys. Today* **April**, 13–15, 81–90 (1993).
2. A. O. Caldeira and A. J. Leggett, *Physica A* **121**, 587 (1983).
3. E. Schrödinger, *Naturwissenschaften* **23**, 807 (1935).
4. A. J. Leggett, *Prog. Theor. Phys. Supplement* **69**, 1 (1980).
5. A. J. Leggett, *Proceedings, International Symposium on Foundations of Quantum Mechanics*, Tokyo, pp. 74–82 (1983).
6. A. J. Leggett and A. K. Garg, *Phys. Rev. Lett.* **54**, 857 (1985).
7. C. Monroe, D. M. Meekhof, B. E. King, and D. J. Wineland, *Science* **272**, 1131 (1996).
8. M. Brune, E. Hagley, J. Dreyer, X. Maitre, A. Maali, C. Wunderlich, J. M. Raimond, and S. Haroche, *Phys. Rev. Lett.* **77**, 4887 (1996).
9. B. Yurke and D. Stoler, *Phys. Rev. Lett.* **57**, 13 (1986).
10. S. Song, C. M. Caves, and B. Yurke, *Phys. Rev. A* **41**, 5261 (1990).
11. A. Montina and F. T. Arecchi, *Phys Rev. A* **58**, 3472 (1998).
12. A. La Porta, R. E. Slusher, and B. Yurke, *Phys. Rev. Lett.* **62**, 28 (1989).
13. B. Yurke, W. Schleich, and D. F. Walls, *Phys. Rev. A* **42**, 1703 (1990).
14. H. Paul, P. Torma, T. Kiss, and I. Jex, *Phys. Rev. Lett.* **76**, 2464 (1996).
15. H. Paul, P. Torma, T. Kiss, and I. Jex, *Phys. Rev. A* **56**, 4076 (1997).
16. G. Breitenbach, S. Schiller, and J. Mlynek, *Nature* **387**, 471 (1997).
17. E. P. Wigner, *Am. J. Phys.* **31**, 6 (1963).